Science Advances
AAAS

Supplementary Materials for

Emergence of the Central Atlantic Niño

Lei Zhang *et al.*

Corresponding author: Lei Zhang, zhanglei@scsio.ac.cn; Chunzai Wang, cwang@scsio.ac.cn

Sci. Adv. **9**, eadi5507 (2023)
DOI: 10.1126/sciadv.adi5507

This PDF file includes:

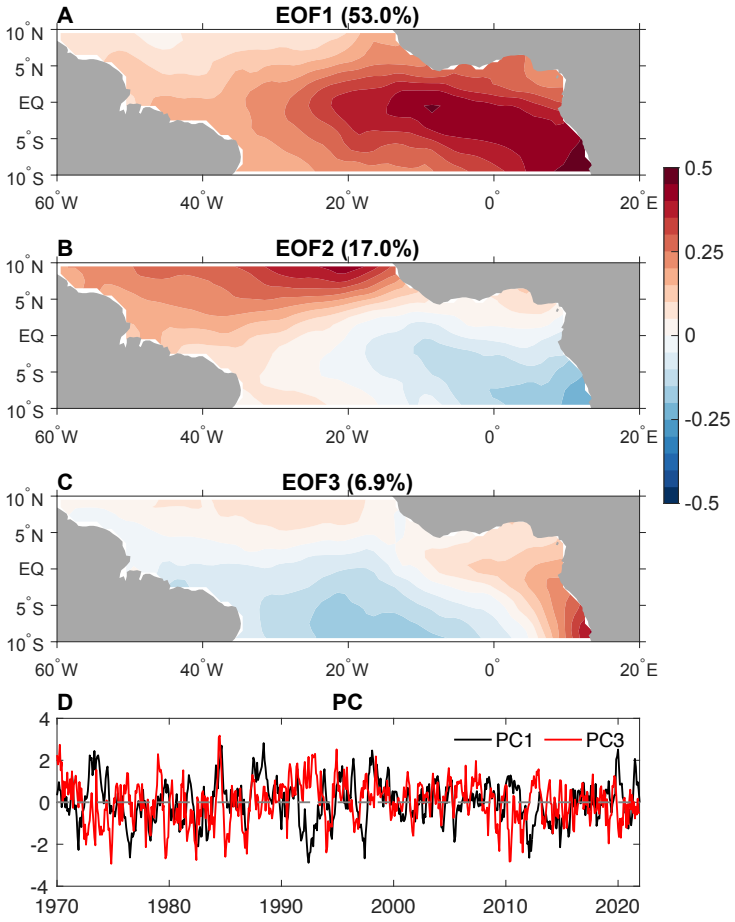

Fig. S1.
(**A**)-(**C**) The first three dominant Empirical Orthogonal Function (EOF) modes. Explained variances are shown in the parentheses. (**D**) Principal components corresponding to the EOF1 and EOF3, i.e., PC1 (black) and PC3 (red).

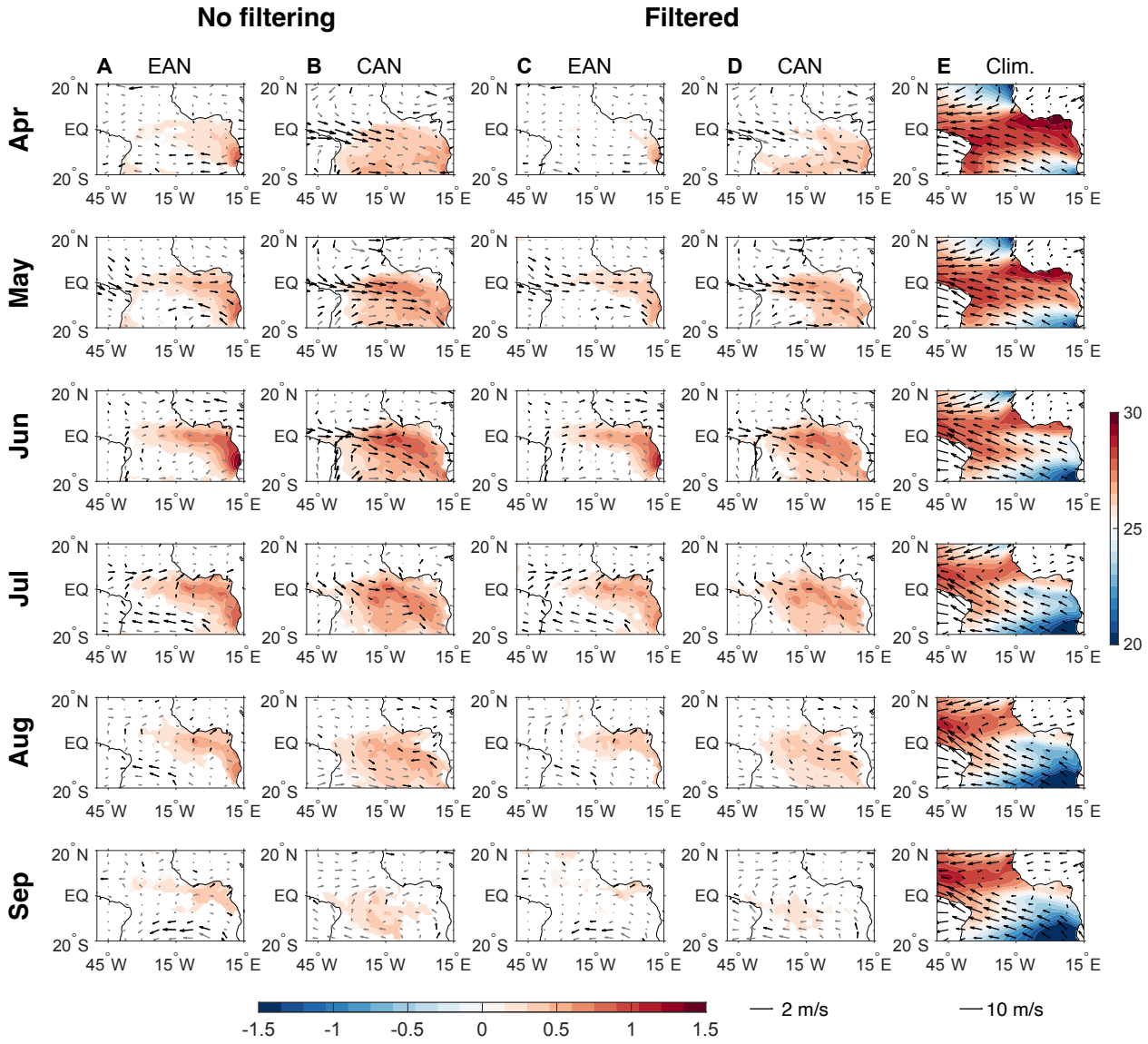

Fig. S2.

Composites of monthly SSTA (shading; ˚C) and 850hPa wind anomalies (vector; m s^{-1}) during the selected (**A**) eastern and (**B**) central Atlantic Niño (see Methods). Shown are differences between Atlantic Niño and Niña events divided by 2. The results are statistically significant at the 90% confidence level. (**C**)(**D**) As in (**A**)(**B**), except for 8-year high-pass filtered results. Climatological SST and winds are shown in (**E**).

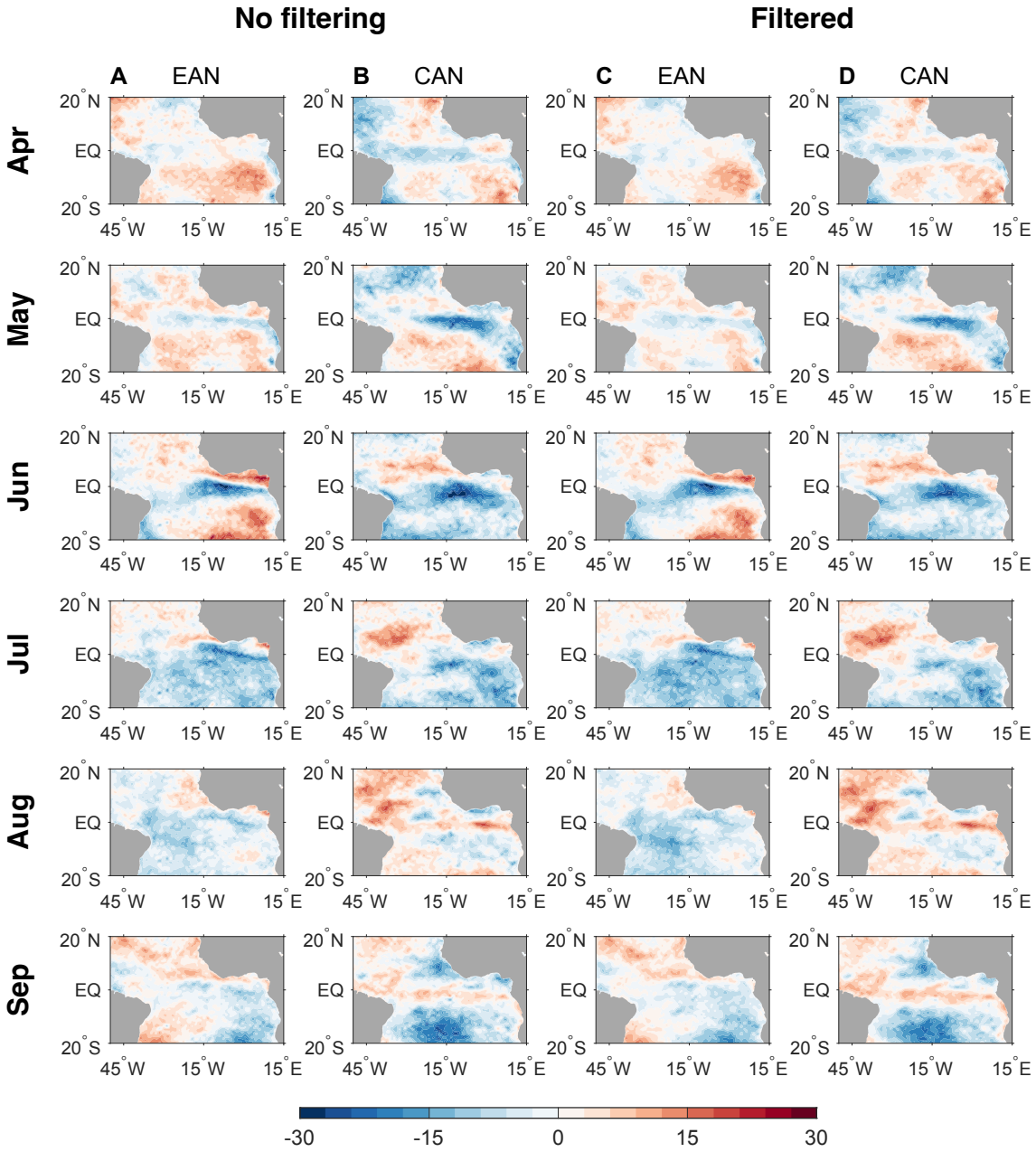

Fig. S3.

Composites of monthly surface net heat flux during the selected (**A**) eastern and (**B**) central Atlantic Niño. Units are W m^{-2}. Shown are differences between Atlantic Niño and Niña events divided by 2. (**C**)(**D**) As in (**A**)(**B**), except for 8-year high-pass filtered results. Negative means ocean loses heat.

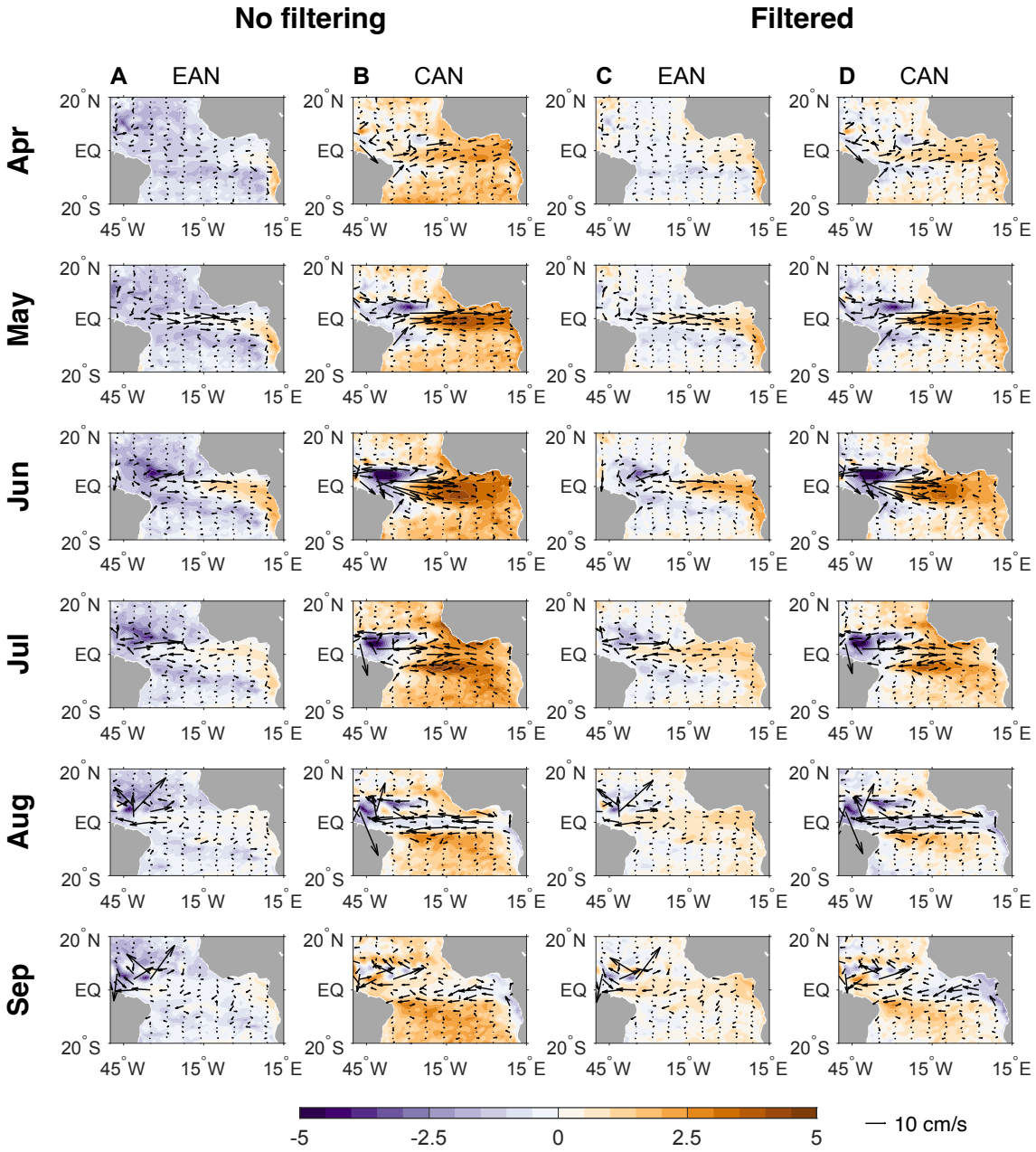

Fig. S4.

Composites of monthly sea level (shading; cm) and ocean current anomalies averaged in the upper 50 m (vector; cm s^{-1}) during the selected (**A**) eastern and (**B**) central Atlantic Niño. Shown are differences between Atlantic Niño and Niña events divided by 2. (**C**)(**D**) As in (**A**)(**B**), except for 8-year high-pass filtered results.

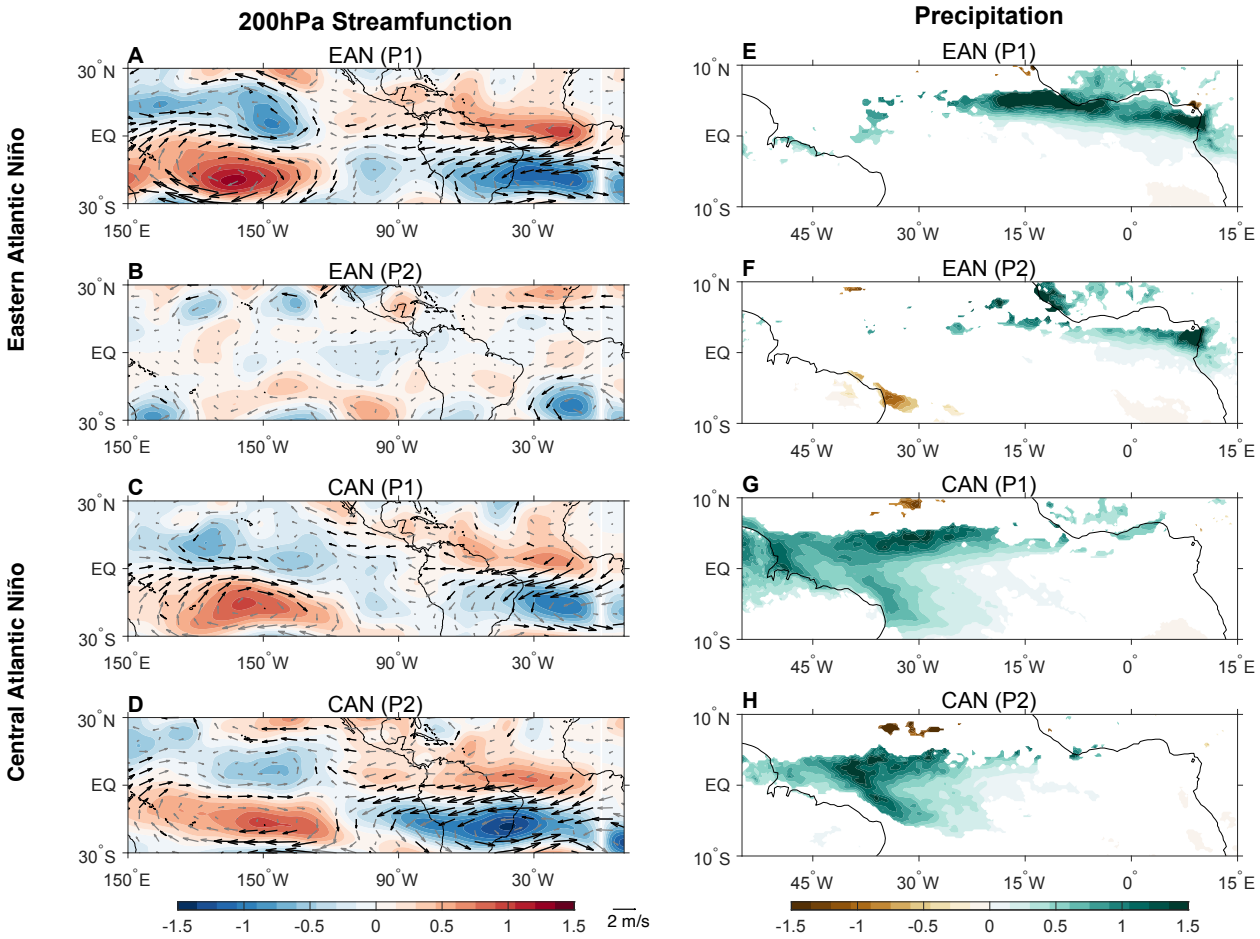

Fig. S5.
(**A**) Regression of JJA mean 200hPa wind (vector; m s^{-1}) and streamfunction anomalies (shading, 10^6 m^2 s^{-1}) on the normalized JJA EANI during 1970-1999. Black vectors denote wind anomalies that are statistically significant at the 95% confidence level. (**B**) Same as (**A**) but for results during 2000-2021. (**C**)(**D**) Same as (**A**)(**B**), except for regression on the normalized JJA CANI. (**E**)-(**H**) As in (**A**)-(**D**), except for regression of JJA mean precipitation anomalies (shading, mm day^{-1}) that are statistically significant at the 90% confidence level.

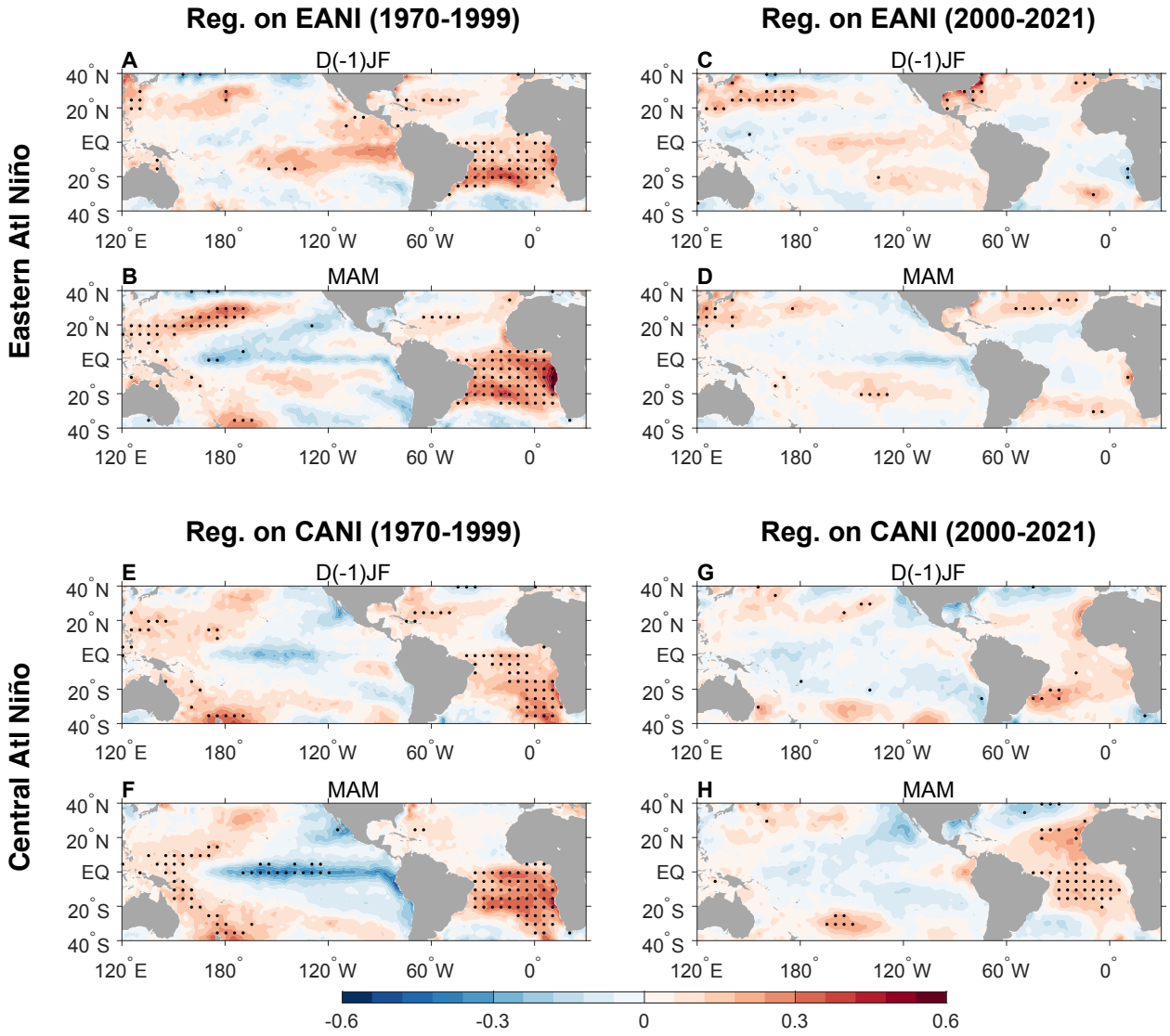

Fig. S6.

(**A**) Regression of D(-1)JF-mean SST (shading, ˚C) and 850hPa wind (vector, m s^{-1}) anomalies on the normalized JJA EANI during 1970-1999. Stippling denotes the results that are statistically significant at the 95% confidence level. (**B**) Same as (**A**), but for regression of the MAM-mean anomalies on the normalized JJA EANI. (**C**)(**D**) Same as (**A**)(**B**), but for results during 2000-2021. (**E**)-(**H**) Same as (**A**)-(**D**), but for regression on the normalized JJA CANI.

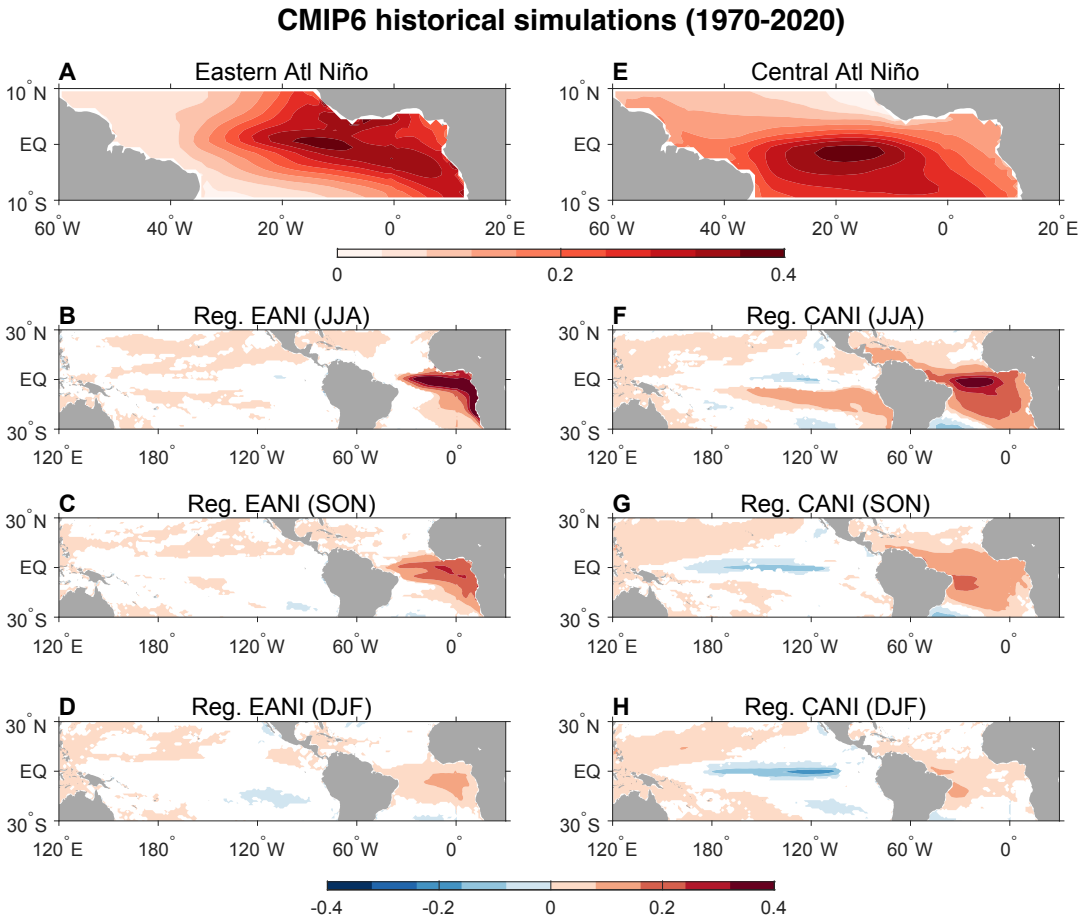

Fig. S7.

(**A**)(**E**) The eastern and the central Atlantic Niño in multi-model mean CMIP6 results (see Methods). (**B**) Multi-model mean regression of JJA SSTA on the normalized JJA EANI. Unit is ˚C. Shown are results in the regions where more than 70% of the models agree on the sign of SSTA. (**C**)(**D**) Same as (**B**), but for regression of the SON and DJF SSTA respectively. (**F**)-(**H**) Same as (**B**)-(**D**), but for regression on the normalized JJA CANI.

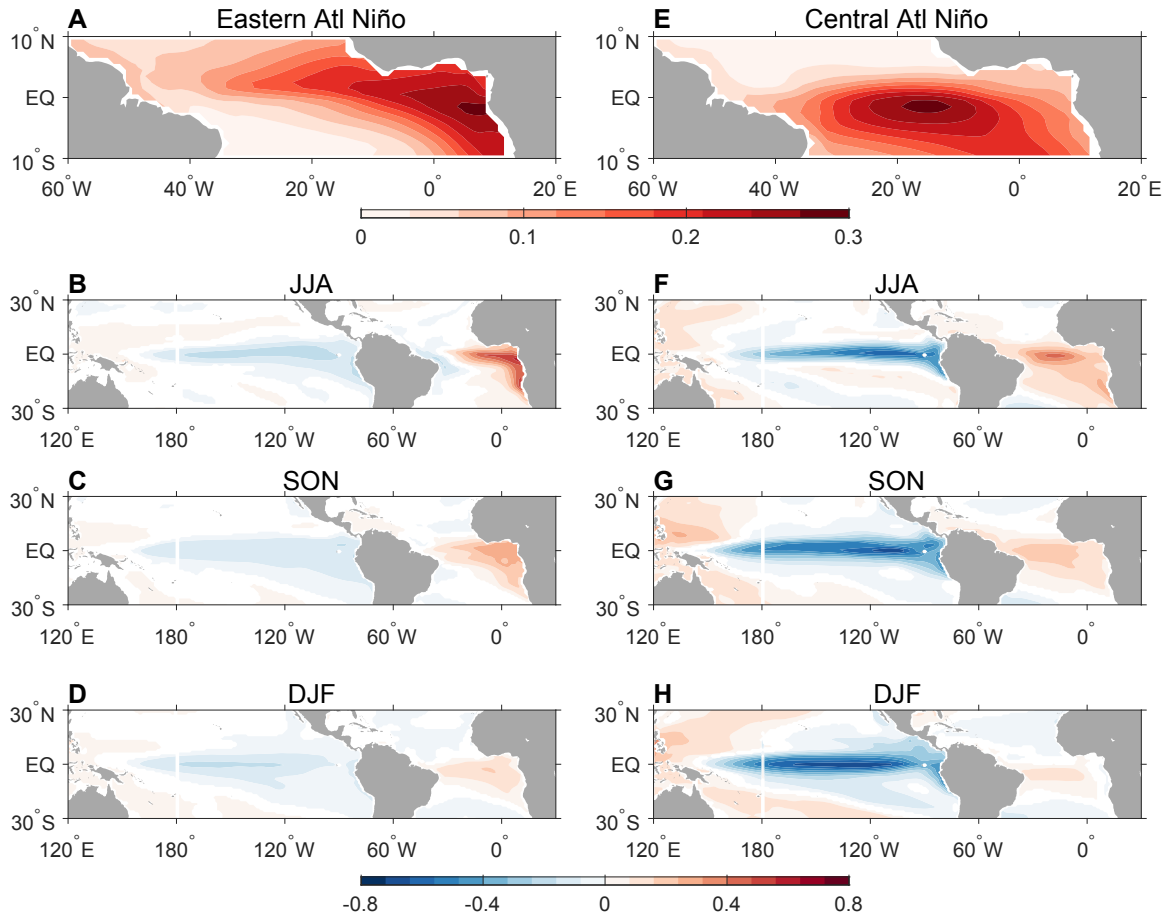

Fig. S8.
(**A**)(**E**) Eastern and central Atlantic Niño in 1300-yr long simulations from one single climate model (see Methods). (**B**) Regression of JJA SSTA on the normalized JJA EANI. Shown are results that are statistically significant at the 95% confidence level. Unit is ˚C. (**C**)(**D**) Same as (**B**), but for regression of SON and DJF SSTA. (**F**)-(**H**) Same as (**B**)-(**D**), but for regression on the normalized JJA CANI.

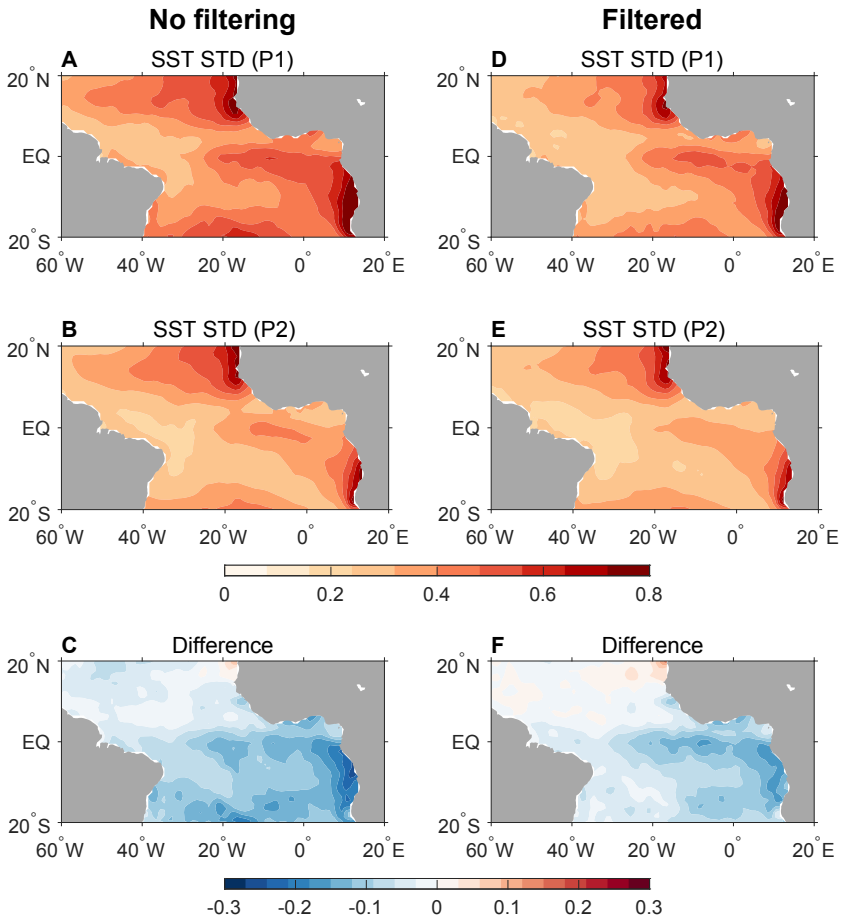

Fig. S9.
Standard deviation of monthly SSTA during (**A**) 1970-1999 and (**B**) 2000-2021. Unit is ˚C. (**C**) Differences between the SSTA standard deviation during the two periods. (**D**)-(**F**) As in (**A**)-(**C**), except for the 8-year high-pass filtered results.

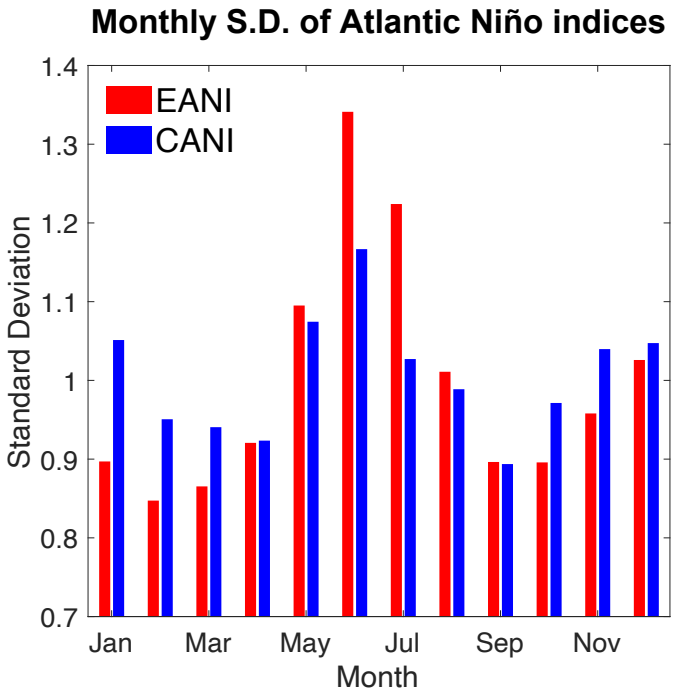

Fig. S10.
Monthly standard deviations of the EANI (red) and the CANI (blue) using HadISST during 1970-2021.

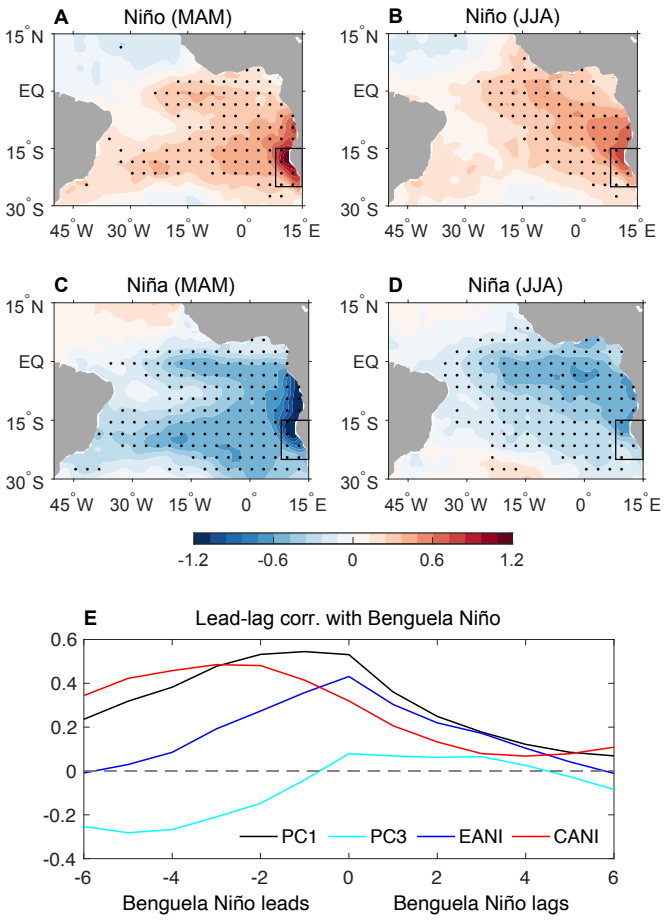

Fig. S11.
Composites of MAM-mean SSTA during the selected (**A**) Benguela Niño years and (**C**) Benguela Niña years. Unit is ˚C. Stippling denotes results that are statistically significant at the 90% confidence level. The boxed region is used to define the Benguela Niño index, which is SSTA averaged over 8˚E-15˚E and 25˚S-15˚S. Benguela Niño/Niña years are then defined as when the MAM-mean Benguela Niño index exceeds (falls below) one standard deviation over the analysis period. (**B**)(**D**) As in (**A**)(**C**), except for JJA-mean SSTA. (**E**) Lead-lag correlation between the Benguela Niño index and PC1 (black), PC3 (cyan), EANI (blue) and CANI (red).

Model	# of ensemble members
ACCESS-CM2	3
ACCESS-ESM1-5	10
CAMS-CSM1-0	2
CMCC-CM2-SR5	1
CMCC-ESM2	1
CNRM-CM6-1-HR	1
CNRM-CM6-1	5
CNRM-ESM2-1	5
EC-Earth3-CC	1
EC-Earth3-Veg-LR	3
FIO-ESM-2-0	1
GFDL-CM4	1
GFDL-ESM4	1
HadGEM3-GC31-LL	4
IITM-ESM	1
MPI-ESM1-2-LR	1
NorESM2-LM	1
NorESM2-MM	1
TaiESM1	1
UKESM1-0-LL	5

Table S1.
20 CMIP6 climate models used in this study. Numbers of ensemble members from each model are shown in the second column. Monthly SST data from all the CMIP6 models are analyzed.